Journal of Molecular Structure 1161 (2018) 1–8

Contents lists available at ScienceDirect

Journal of Molecular Structure

journal homepage: http://www.elsevier.com/locate/molstruc

Crystal structures and molecular dynamics studies of the inclusion compounds of β-citronellol in β-cyclodextrin, heptakis(2,6-di-*O*-methyl)-β-cyclodextrin and heptakis(2,3,6-tri-*O*-methyl)-β-cyclodextrin

Katerina Fourtaka, Elias Christoforides, Dimitris Mentzafos, Kostas Bethanis*

Physics Laboratory, Department of Biotechnology, Agricultural University of Athens, Iera Odos 75, 11815 Athens, Greece

ARTICLE INFO

Article history:
Received 19 December 2017
Received in revised form
5 February 2018
Accepted 8 February 2018
Available online 10 February 2018

Keywords:
β-citronellol
β-cyclodextrin
Methylated β-cyclodextrin
Inclusion complex
Crystal structure
Molecular dynamics

ABSTRACT

The crystal structures of the inclusion complexes of the β-citronellol (*cl*) inβ-Cyclodextrin (β-CD), heptakis(2,6-di-*O*-methyl)-β-Cyclodextrin (DM-β-CD) and heptakis(2,3,6-tri-*O*-methyl)-β-Cyclodextrin (TM-β-CD) have being investigated by X-ray crystallography. The *cl*/β-CD inclusion complex crystallizes in the *P*1space group forming dimers which are arranged along the *c*-axis according to the Intermediate Channel packing mode. Inside the dimeric host cavity two enantiomeric guest molecules are accommodated. The inclusion complexes of *cl*/DM-β-CD and *cl*/TM-β-CD crystallize in the $P2_12_12_1$ space group having both 1:1 guest:host stoichiometry, the guest found always with the (−)-*cl* enantiomeric configuration. The guest is fully encapsulated inside the DM-β-CD host cavity whereas is partially encapsulated in the TM-β-CD which is severely puckered as in all TM-β-CD complexes and its primary side is efficiently blocked by the methoxy groups. The complex units in the case of *cl*/DM-β-CD pack along the crystallographic *a*-axis in a head-to-tail manner forming columns of herringbone mode whereas in the case of *cl*/TM-β-CD are arranged also head-to-tail, parallel to the *b*-axis, in a screw-channel mode.

MD simulations based on the determined crystal structures showed that in a simulated aqueous environment the guest maintains the inclusion mode observed crystallographically in every case. MM/GBSA-calculations used for comparison of the inclusion complexes binding affinity with each other, indicated that the inclusion of β-citronellol in TM-β-CD is less favorable than in β-CD and DM-β-CD.

1. Introduction

Mosquitoes are insects of major public health concern as their bites may cause allergic responses and transmit life threatening diseases [1] and thus the use of mosquito repellents is necessary. There is a variety of mosquito repellents which are classified into two categories: synthetic and natural. Most of the synthetic anti-mosquito products contain DEET (diethyl-meta-toluamide), a compound that causes risks to human health and environment. On the other hand, various essential oils have been reported as mosquitoes' repellents having an eco-friendly and biodegradable nature [2]. Citronella oil which is mainly constituted by β-citronellol, geraniol and citronellal is a natural insect repellent [3], considered to be safe and more suitable for small children [4]. However, citronella oil should not be directly applied onto the skin as it may cause skin irritation and sensitization [5]. β-citronellol (*cl*) or dihydrogeraniol (3,7-Dimethyl-6-en-1-ol) is a natural acyclic monoterpenoid occurring in two enantiomeric modes (+)- and (−)-*cl* (Fig. 1a and b). Although it has been traditionally used as a mosquito repellent, its high volatility leads to a short-lasting protection. Among other techniques that can eliminate this disadvantage and increase their repellent efficiency (polymer mixtures, microcapsules, nanoemulsion etc) [4], the encapsulation of these substances into cyclodextrins (CDs) is an effective and common used method.

CDs are able to incorporate apolar molecules (guests) or parts of molecules inside their hydrophobic cavity resulting in better stability, higher water solubility and increased bioavailability or decreased undesirable side effects of the hydrophobic molecules.

Abbreviations: β-citronellol, *cl*; Beta-cyclodextrin, β-CD; 2,6-di-*O*-methyl-β-CD, DM-β-CD; 2,3,6-tri-*O*-methyl-β-CD, TM-β-CD.

* Corresponding author.
E-mail address: kbeth@aua.gr (K. Bethanis).

https://doi.org/10.1016/j.molstruc.2018.02.037
0022-2860/

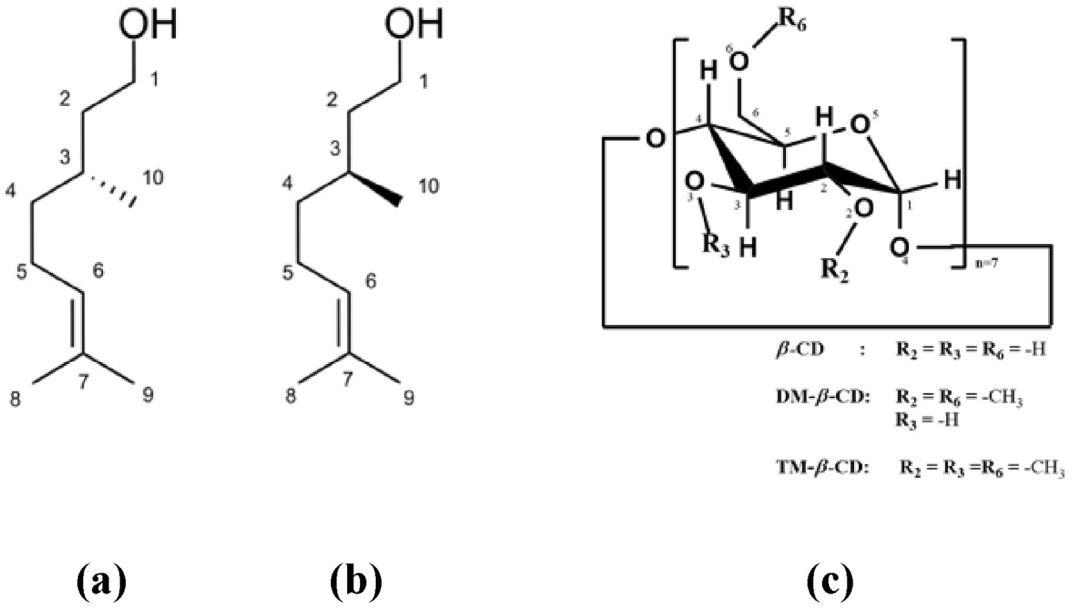

Fig. 1. Schematic representation of **(a)** (+)-*cl*, **(b)** (−)-*cl*, **(c)** β-CD, DM-β-CD and TM-β-CD.

Moreover, they offer a slow release of the guests sustaining their action. Although β-CD(Fig. 1c) is the less soluble cyclodextrin in water, it is the most popular member of CDs for several applications due to its cavity size and its low cost. Methylated CDs (Fig. 1c) are commercially available CD derivatives having improved physicochemical properties and inclusion capacity compared to the parent CDs [6]. The formation and study of inclusion complexes in methylated CDs is also of interest as they present enhanced aqueous solubility and can modulate the release rates of the guest molecules.

The inclusion of (+)- and (−)-*cl* in β-CD has been previously studied in solid state by Fourier Transform Infrared Spectroscopy (FTIR), Scanning Electron Microscopy (SEM) and Differential Scanning Calorimetry (DSC) [4]. Evolved gas detection and TG-MS coupling has also been applied to prove the actual inclusion complex formation between citronellol and α-, β- and γ-CDs whereas predictions of their inclusion modes and compositions have been given by molecular modeling calculations [7]. However, the structure of these inclusion compounds has not been determined yet. Crystallographic analysis offers a detailed description of the formed inclusion complexes (stoichiometry, inclusion geometry, etc.) in the crystalline state. In this work we present the crystal structures of the inclusion compounds of *cl* in β-CD, 2,6-di-*O*-methyl-β-CD (DM-β-CD) and 2,3,6-tri-*O*-methyl-β-CD (TM-β-CD) as determined by X-ray crystallography. Moreover, based on the crystallographically determined atomic coordinates, molecular dynamics (MD) simulations were performed for the three inclusion compounds with the aim to monitor the dynamic behavior of *cl* in different hosts, study the different inclusion modes and calculate the host-guest binding affinity in each case.

2. Materials and methods

2.1. Materials

The enantiomeric mixture of β-citronellol ((+)- and (−)-*cl*), β-CD, DM-β-CD and TM-β-CD were obtained from Sigma-Aldrich and used as received (commercially available products of analytical grade).

2.2. Sample preparation

Crystals of the inclusion compound of *cl*/β-CD were formed by using the slow cooling crystallization technique. 17 μL of enantiomeric mixture of β-citronellol (d = 0.857 g/mL) were added in a 5 mL aqueous solution of β-CD (0.08 mmol, ~0.016 M), stirred at 70 °C for 1 h and the final mixture was gradually cooled to room temperature over a period of seven days. Crystals of *cl*/DM-β-CD and *cl*/TM-β-CD complex were obtained by adding suitable amounts of enantiomeric mixture of β-citronellol in a 0.3 M aqueous solution of DM-β-CDor a 0.05 M aqueous solution of TM-β-CD in a host:guest molar ratio of 1:1, respectively. The final mixtures were stirred at room temperature for 30 min and then were maintained in a water bath at 48 °C until colorless transparent prismatic crystals were formed. X-ray data were collected from crystals of these three inclusion compounds under cryo-conditions using paraffin oil as cryoprotectant.

2.3. X-ray data collection, structure solution and refinement

The X-ray data were collected at 100(2) K on a Bruker D8-VENTURE diffractometer, using Cu*Ka* radiation (λ = 1.54178 Å) and an Oxford Cryosystems low-temperature device. Data integration and global-cell refinement was performed with the program *SAINT* [8]. Absorption correction was performed with *SADABS* [9]. The structures have been solved by Patterson-seeded dual-space recycling in the *SHELXD* program [10] refined by full-matrix least squares against F^2 using *SHELXL-2014/7* [11]through the *SHELXLE GUI* [12]. Due to the limited resolution and structural complexity of the model, soft restraints on bond lengths and angles of the host and guest molecules were applied using the *PRODRG2* webserver [13]. Anisotropic displacement parameters were refined using the rigid bond restraint (RIGU) implemented in the *SHELXL* program [14]; SIMU and DELU restraints were also applied where necessary. All H-atoms of the host molecules were placed geometrically for temperature of 100 K and allowed to ride on the parent atoms. *U*iso(H) values were assigned in the range 1.2−1.5 times *U*eq of the parent atom. In order to maintain a high (>8.0) data/parameters ratio, anisotropic thermal parameters were imposed to selected, non-H

Table 1
Experimental details, crystal data and refinement statistics.

	cl/*β*-CD	*cl*/DM-*β*-CD	*cl*/TM-*β*-CD
Chemical formula	$2[C_{42}H_{70}O_{35}]\cdot 2[C_{10}H_{20}O]$	$C_{56}H_{98}O_{35}\cdot C_{10}H_{20}O$	$C_{63}H_{112}O_{35}\cdot C_{10}H_{20}O$
M_r	1449.12	1505.23	1571.91
Crystal system space group	Triclinic	Orthorhombic	Orthorhombic
	*P*1	$P2_12_12_1$	$P2_12_12_1$
Temperature (K)	100	100	100
a, *b*, *c* (Å)	15.383 (2), 15.409 (2), 17.713 (2)	10.391 (3), 15.1063(18), 51.050 (8)	14.9291 (19), 20.947 (3), 27.683 (4)
αβ, *γ* (°)	113.898 (9), 99.431 (9), 102.109 (9)		
V (Å^3)/*Z*	3604.9 (9)/2	8013 (3)/	8657 (2)/
Radiation type	Cu*Kα*	Cu*Kα*	Cu*Kα*
Crystal size (mm)	0.5 × 0.44 × 0.18	0.5 × 0.3 × 0.2	0.1 × 0.08 × 0.05
$(\sin\theta/\lambda)_{max}$ (Å^{-1})	0.618	0.550	0.510
Reflections collected	70467	80357	39739
Limiting indices	$-18 \le h \le 18$	$-11 \le h \le 11$	$-15 \le h \le 15$
	$-19 \le k \le 16$	$-16 \le k \le 16$	$-21 \le k \le 16$
	$-21 \le l \le 21$	$-56 \le l \le 56$	$-28 \le l \le 28$
Independent, observed reflections[$I > 2\sigma(I)$]	25966/25329	11133/10595	9129/8745
R_{int}	0.047	0.045	0.074
Goodness-of-fit	0.92	1.07	1.14
$R[F^2 > 2\sigma(F^2)]$ $wR(F^2)$	0.079	0.093	0.089
	0.219	0.255	0.242
No. of parameters/restraints	1243/163	882/66	883/33
Largest difference peak and hole (e Å^{-3})	0.89, −0.75	0.75, −0.51	0.67, −0.60

atoms of the host molecules. The graphics programs used to illustrate and geometrically analyze the crystal structures are Mercury 3.9 [15] and Olex2 [16]. Crystallographic data are given in Table 1. Crystallographic information files with embedded structure factors have been deposited into the Cambridge Structural Database (CSD) under the deposition numbers CCDC: 1574446, 1575058, 1574710.

2.4. Molecular dynamics

The Amber12 suite [17] was used for the 12 ns simulations, with the most recent parametrization of the AMBER related additive force fields, CLYCAM [18] and q4md-CD [19] for native *β*-CD and methylated *β*-CD (DM-*β*-CD and TM-*β*-CD) atoms, respectively. The starting atomic coordinates for all simulations were taken from the crystallographically determined structures of *cl*/*β*-CD, *cl*/DM-*β*-CD and *cl*/TM-*β*-CD inclusion complexes. GAFF parameters and AM1BCC charges were applied to the guest enantiomers using ANTECHAMBER [20].

Each complex was solvated by explicit waters and hydrogen atoms were added with xLEaP in all systems. The “solvateoct” command of xLEaP was utilized to create a periodic, octahedral solvent box around the solutes with buffer distances of 10.0 Å between the walls of the box and the closest atoms of the solute.

MD calculations and minimizations were carried out with the program SANDER. Periodic boundary conditions were imposed by means of the particle mesh Ewald method using a 10 Å limit for the direct space sum. The protocol included energy minimization for hydrogen atoms with positional restraints of 50 kcal mol^{-1} Å^{-2} on the non-hydrogen atoms, heating equilibration of the solvent in the canonical ensemble (NVT) using positional restraints and the Berendsen thermostat algorithm with coupling constants of 0.5 ps to control temperature and pressure, unrestrained energy minimization, gradual temperature increase from 5 to 300 K with 10 kcal mol^{-1} Å^{-2} restraints on the atoms of the inclusion complex, gradual release of the restraints in successive steps at 300 K and density equilibration in the isobaric-isothermal (NPT) ensemble for 250 ps. Subsequently, production runs using a Berendsen-type algorithm with coupling constants of 1.0 ps were carried out under physiological conditions for additional 11 ns in the NPT ensemble. Root mean square deviation (RMSD) calculations and geometric analysis were performed by CPPTRAJ [21] and VMD 1.9.2 [22].

Moreover, the binding free energy $\Delta G_{(GB)}$ between the bound and unbound state of the solvated host and guest molecules energy for each complex was computed also by the MM/GBSA (Molecular Mechanics-Generalized Born/Surface Area (LCPO)) methodology implemented in AMBER [23], in order to compare the binding affinities between inclusion complexes. $\Delta G_{(GB)}$ value includes the van der Waals contribution from molecular mechanics, the electrostatic energy calculated by the molecular mechanics force field, the electrostatic contribution to the solvation free energy calculated by the G_B model and the nonpolar contribution to the solvation free energy calculated using 'LCPO′ surface areas. In order to estimate the absolute binding free energy $\Delta G_{(all)}$, the entropy term $T\cdot\Delta S$ was also calculated from normal mode analysis with constant temperature using the respective module of the Amber 12 suite and added to the $\Delta G_{(GB)}$ term according to:

$$\Delta G_{(all)} = \Delta G_{(GB)} - T\cdot\Delta S$$

The entropy term was calculated by taking snapshots every 100 frames for as long as the equilibrated system of the inclusion complex was subjected to MD simulations. However, it should be noted that the estimation of the entropy term is often problematic as the normal mode lacks information of the conformational entropy and alternative methods do not give converged results [24]. Thus, this term is usually omitted and the comparison of binding affinities between similar complexes is based on the $\Delta G_{(GB)}$ term solely.

3. Results and discussion

3.1. Description of the crystal structures

3.1.1. The *cl*/*β*-CD inclusion complex

The *cl*/*β*-CD inclusion complex crystallizes in *P*1 space group and its asymmetric unit contains two *β*-CD host molecules (hostA and hostB), a couple of *cl* enantiomeric guest molecules and 25 water molecules distributed over 29 sites. The two host molecules are arranged co-axially so that the secondary wide rim (head) of the one faces the secondary rim of the other forming a head-to-head dimer via intermolecular hydrogen bonds between their O3*n*H hydroxyl groups (Fig. 2a). Both enantiomeric configurations of *cl* are

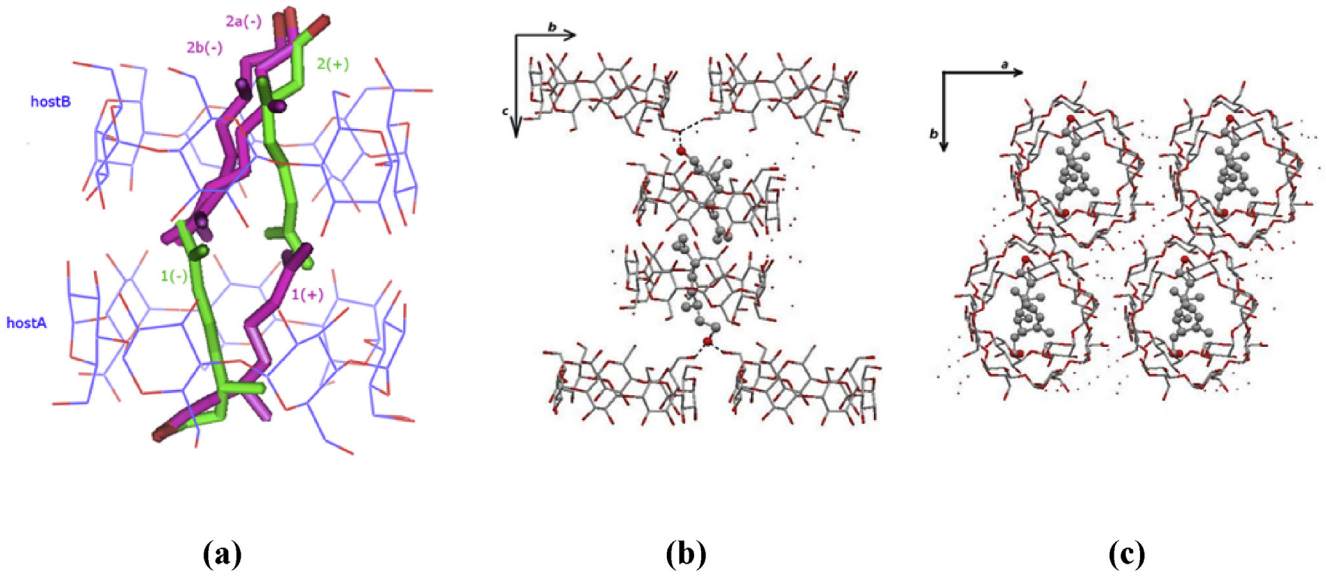

Fig. 2. (a) The *cl*/*β*-CD inclusion complex forms a 'classical' head-to-head dimer with a host:guest stoichiometry of 2:2. Water molecules are omitted for clarity. **(b), (c)** projection of the crystal packing along *a*- and *c*-axis respectively.

found inside the hostA cavity (sites denoted as 1(+) and 1(−)), having an occupation factor of 0.5 each. Inside the hostB cavity, the two enantiomeric configurations are also present, with one of them (site denoted as 2(+)), having an occupancy factor of 0.5 whereas the other, 2(−), is found disordered over two sites: 2a(−) and 2b(−) with occupancy factors of 0.3 and 0.2 respectively. Due to steric reasons indicated by the geometrical features of the occupied sites, the encapsulated guests can co-exist only as 1(−)/2(+) or 1(+)/2a,b(−) couples. The estimated occupancy factors are in accordance with this observation. Thus in every case, a couple of enantiomers is hosted inside the *β*-CD dimeric cavity forming an inclusion complex of 2:2 host:guest stoichiometry in the crystalline state. The guest molecules are accommodated axially inside the dimeric cavity with their long axis (mean axis along O1—C1—C2—C3—C4—C5—C6—C7 atoms, see Fig. 1a and b, 2a) forming angles with the approximate seven-fold molecular axis of the host that range between 1.3° and 25.5°. The hydrophobic alkyl groups of the guests are located in the interface of the dimer, their C8 or C9 methyls forming closed shell interactions with the inner H3 atoms of the *β*-CD hydrophobic cavity. The hydroxyl groups of the guests protrude from the primary host regions (Fig. 2a) connected to the hosts of adjacent inclusion complexes either directly, via hydrogen bonds with their primary hydroxyls (Fig. 2b), or indirectly via hydrogen bonds with bridging water molecules (main hydrogen bonds are listed in supplementary file, Table S1).

Geometrical features defining the conformation of the host molecules are listed in supplementary Table S2. The glucosidic O4*n* atoms in both host molecules form nearly regular heptagons as indicated by their distances from their approximate centroids and their deviations from the O4*n* mean plane. The glycosidic residues have positive tilt angles indicating that their primary sides incline towards the approximate sevenfold axis of the cavity. Almost all the primary hydroxyl groups of both hosts A and B have the *gauche-gauche (gg)* conformation pointing outwards the cavity, hydrogen bonded with bridging water molecules. Only one disordered primary hydroxyl in each host has the *gauche-trans* (gt) conformation pointing inwards the cavity.

The *β*-CD dimers stack along the *c*-axis and form layers along the *ab* crystal plane (Fig. 2b and c). Their approximate seven-fold axis forms an angle of 20.07° with the *c*-axis. The shift between successive dimers along the *c*-axis is 5.93 Å. This displacement is very close to the average value of 6 Å observed in the case of the dimeric structures crystallizing according to the Intermediate Channel (*IM*) packing mode [25]. This well-known packing arrangement has been observed in numerous isostructural dimeric *β*-CD inclusion complexes [26]. Among them the structure of geraniol/*β*-CD [27] has many similarities with *cl*/*β*-CD as in both cases the acyclic monoterpenoid guest is encapsulated in the same manner in the cavity of *β*-CD dimers that stack along *c*-axis forming *IM* channels. On the other hand, linalool, which is also a linear monoterpenoid alcohol, forms inclusion complexes with *β*-CD dimers that stack along *a*-axis forming screw channels as the vinyl group and the position of the hydroxyl group of linalool affect the arrangement of successive dimers and thus the crystal packing of the inclusion complex [28].

3.1.2. The cl/DM-β-CD inclusion complex

The complex crystallizes in the orthorhombic space group $P2_12_12_1$ and its asymmetric unit contains one host molecule and one *cl* guest molecule, disordered over two sites, (−) a and (−) b, of occupancy factor 0.5 each, both sites having the (−)-*cl* configuration. Thus, the host:guest stoichiometry of the inclusion complex is 1:1. Furthermore, 4.3 water molecules have been located and distributed over 7 sites, with fractional sof's (0.3—1). The guest molecule in both occupied sites is fully encapsulated into the DM-*β*-CD cavity with its hydroxyl and its alkyl group located in the primary and secondary region of the host respectively (Fig. 3a). The accommodation of the guest in the hydrophobic cavity of the host is arranged mainly via C—H…O bonds and H…H closed shell interactions between its alkyl group (atoms C8 and C9) and the secondary rim of the host whereas only a C—H…O bond between a disordered primary methoxy group of the host and the hydroxyl group of the (−) a occupied site of the guest is observed in the crystalline state.

The host DM-*β*-CD cavity is stabilized by the commonly observed intramolecular O3(*n*) … O2(*n*+1) hydrogen bonds in the crystalline state. The geometrical features of DM-*β*-CD quoted in supplementary Table S3, indicate a host macrocycle that is close to a regular heptagon similar to that of native *β*-CD. All the methoxy-glycosidic residues have positive tilt angles, indicating that their

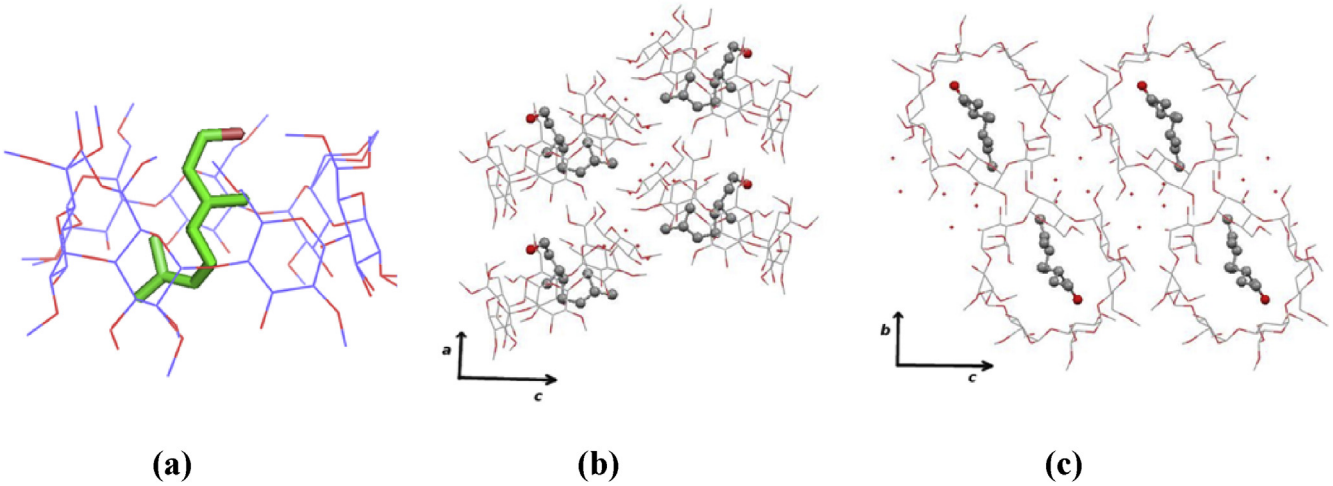

Fig. 3. (a) The asymmetric unit of (−) *cl*/DM-*β*-CD inclusion compound **(b), (c)** projections of the crystal packing along *b*- and *a*-axis respectively, only one of the two guest's occupied sites is drawn for clarity.

primary sides incline towards the approximate sevenfold axis of the host's macrocycle. Among the five fully occupied primary methoxy sites, 3 of them are found to have the *gg* conformation and two the *gt* conformation pointing outwards and inwards the host's cavity respectively. The two disordered methoxy groups have both *gt* and *gg* conformations. Therefore, the host is characterized by an open truncated cone conformation which allows the guest to protrude from its primary rim.

The complex units stack in columns parallel to the *a*-axis in a head-to-tail fashion. The displacement of two successive complexes of the same column is 5.32 Å and the distance between them 8.92 Å. In this motif, two successive host molecules are inclined to the *a*-axis, their O4n mean plane forming an angle of 30.87° with *bc* plane, so that two primary methoxy groups of the uppermost molecule are partially included within the cavity of the translated molecule. The angle between the O4n mean planes of the hosts of adjacent columns is 61.73° forming a herringbone crystal packing (Fig. 3b and c). The water molecules located in the interspace of the inclusion complexes are hydrogen bonded with the O6*n*oxygen atoms of the primary methoxy groups of the host and with secondary hydroxyls of neighboring hosts bridging the adjacent columns and aiding the crystal packing. (supplementary Table S1 and Fig. 3b and c). The *cl*/DM-*β*-CD is isostructural to the *trans*-resveratrol/DM-*β*-CD inclusion complex [29] which crystallizes in the same space group with similar unit cells and also according to a herringbone packing arrangement. The similarity in the crystal packing of the above inclusion complexes is interesting as *trans*-resveratrol is a bulky guest molecule and its 1,3-benzenediol residue protrudes from the secondary rim of the host, laying in the interspace of the complex units, whereas *β*-citronellol is fully encapsulated in the DM-*β*-CD cavity. Closer examination of the mode that complex units stack in columns in both cases, reveals the same extent of self-inclusion between successive hosts as described above. Therefore, it seems that DM-*β*-CD self-inclusion tendency can drive to the same packing arrangement inclusion complexes with guests of different size and inclusion geometry.

3.1.3. *The cl/TM-β-CD inclusion complex*

The *cl*/TM-*β*-CD inclusion complex crystallizes in the orthorhombic space group $P2_12_12_1$. Its asymmetric unit contains one TM-*β*-CD molecule, one guest molecule and one water molecule having an occupancy factor of 0.50. The guest molecule is accommodated

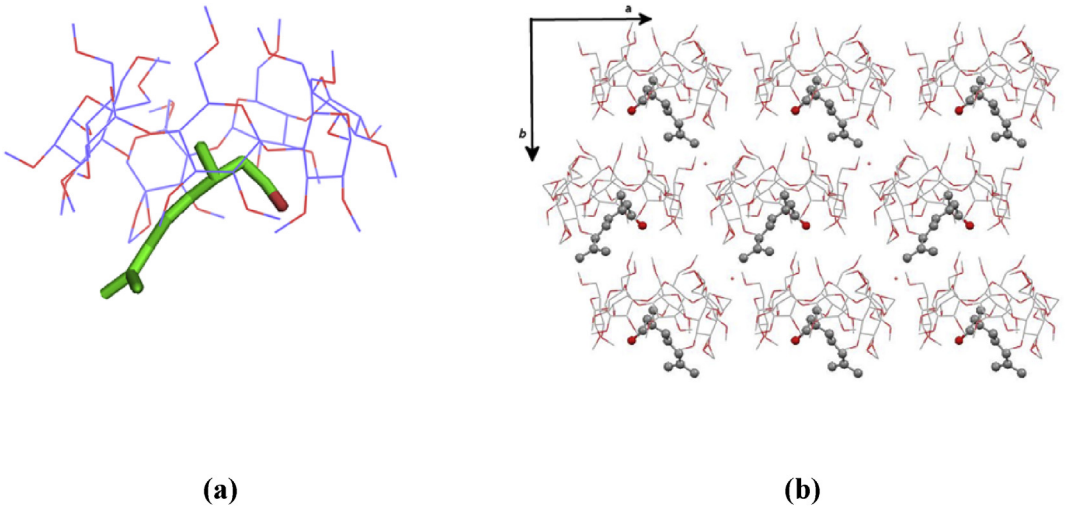

Fig. 4. (a) The asymmetric unit of *cl*/TM-*β*-CD **(b)** A packing diagram of the inclusion complex *cl*/TM-*β*-CD viewed along *c*-axis.

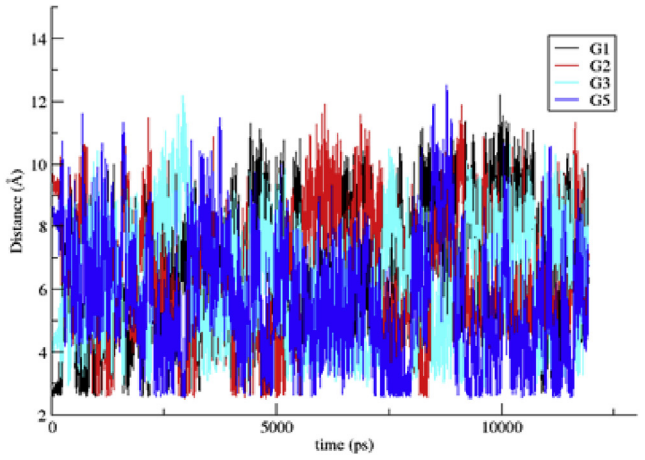

(a)

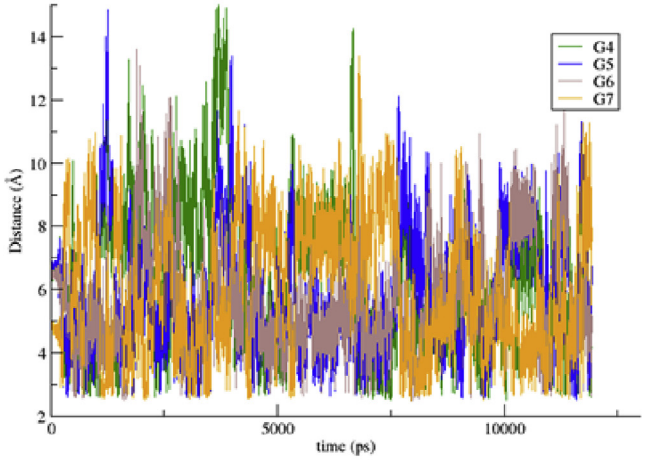

(b)

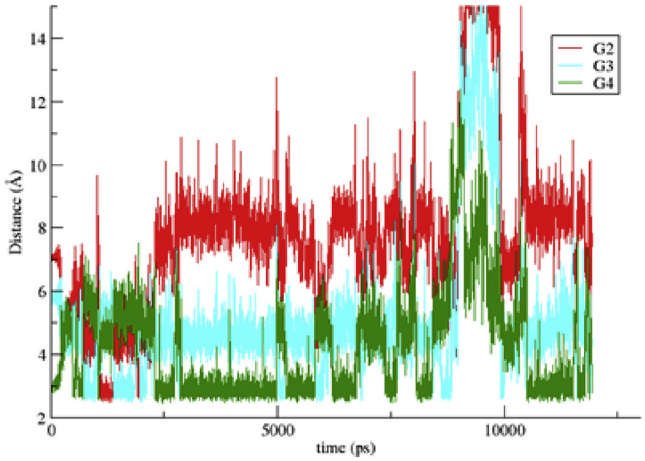

(c)

in the host's cavity having a different orientation compare to that observed in the cases of *cl* inclusion complexes in *β*-CDand DM-*β*-CD. Its hydroxyl group is located in the wide rim of the host, forming a hydrogen bonded with the O24 atom of the host's secondary methoxy group (O1A … O24 distance 2.90(2) Å) and a C—H…O bond with a primary methoxy group of a neighboring TM-*β*-CD (C75—H75A$^{(i)}$ … O1 distance 2.67(2) Å; i: −0.5 + x, 0.5−y, 1−z). Its aliphatic tail protrudes from the secondary rim of the host and is mainly located in the interspace of adjacent inclusion complexes (Fig. 4a and b). The sole, partially occupied, water molecule is found hydrogen bonded with the O54 atom of TM-*β*-CD (OW1 ⋯ O54 = 2.81(3) Å).

The conformation of the TM-*β*-CD host molecule is quite different than that of the hosts in the cases of the *cl*/*β*-CD and *cl*/DM-*β*-CD complexes. Geometrical parameters regarding TM-*β*-CD conformation are given in supplementary Table S4. The glucosidic O4n atoms deviate noticeably from their mean plane forming an elliptical heptagon. Thus, the host molecule is severely distorted, a feature commonly observed in the crystal structures of the TM-*β*-CD inclusion complexes due to the absence of the intramolecular hydrogen bonds between the secondary methoxy groups. The observed methylglucose ring tilt angles span a very wide range, from −15.58(4)° (for G5) to 40.53(7)° (for G4). Five residues have positive tilt angles indicating that their primary sides incline towards the approximate sevenfold axis of the macrocycle whereas two methyl-glucose residues (G2 and G5) have negative tilt angles inclining outwards the host cavity. This is also a common feature to the majority of the TM-*β*-CDcomplexes. Moreover, the O5*n*-C5*n*-C6*n*-O6*n* torsion angles indicate the *gg* conformation for all primary methoxy groups except for two partially disordered sites where the gauche-trans (*gt*) and the trans-gauche *(tg)* conformation is observed. These features resulted in the formation of a 'lid' in the primary region of the host, a characteristic usually observed inTM-*β*-CD inclusion complexes [30], that prevents the deep penetration of the guest.

The complex units pack in a screw-channel mode and are arranged in a head to-tail manner parallel to the *b*-axis (Fig. 4b). The shift between alternate host molecules in a particular column is 3.94 Å. Parallel and anti-parallel columns are arranged along *a*- and *c*-axis respectively, stabilized primarily by a large number of intermolecular host C—H …O(host) bonds and completing a fairly commoncrystal packing that characterizes several other isostructural TM-*β*-CD complexes [26].

3.2. Molecular dynamics

The crystallographically determined atomic coordinates of *cl*/*β*-CD, *cl*/DM-*β*-CD and *cl*/TM-*β*-CD inclusion complexes (host:guest ratio 2:2, 1:1 and 1:1, respectively) were subjected to equilibration and subsequent molecular dynamics simulations at 300 K in explicit water solvent for almost 12 ns as described in paragraph 2.4.

In the case of *cl*/*β*-CD, the starting model comprises of a duet of guests having different enantiomeric configuration, guest 1(−) and 2(+), encapsulated in a head-to-head *β*-CD dimer. By monitoring the frames during the time interval of the simulation, we observed that the guest molecules rotate about the seven-fold molecular axis of the hosts retaining their initial orientation in a stable *β*-CD dimer. The hydroxyl groups of the guests are almost always hydrogen

Fig. 5. Plots of H-bond distances between the O1 atom of the hydroxyl group of the *β*-citronellol guest and (**a**) O6*n* atoms of the primary hydroxyls of selective glucopyranose units of *β*-CD (case of 1(−) in hostA), (**b**) O6*n* atoms of the primary methoxy groups of selective glucopyranose units of DM-*β*-CD (**c**) O2*n* atoms of the secondary methoxy groups of selective glucopyranose units of TM-*β*-CD.

bonded with alternate primary hydroxyls of the hosts (Fig. 5a) whereas their alkyl groups, located in the interface of the dimer, form closed-shell weak H…H interactions with the inner hydrogens (H3*n*) of the secondary rim of the hosts.

In the case of 1(−)/DM-*β*-CD, the guest molecule remains encapsulated 'axially' inside the hydrophobic DM-*β*-CD cavity during the 12 ns simulation rotating about the seven fold molecular axis of the host. As DM-*β*-CD retains its open cone conformation, the hydroxyl group of the guest projects always through the host's primary rim forming hydrogen bonds with oxygens of alternate primary methoxy groups and water molecules (Fig. 5b). The depth of immersion of the guest in the hydrophobic cavity of the host varies accordingly. Its alkyl group is located in the secondary rim of the host when its hydroxyl group is hydrogen bonded with a host's primary methoxy group whereas is deeply immersed in the hydrophobic cavity of the host when the hydroxyl of the guest forms H-bonds with solvent water molecules.

On the other hand, in the case of 1(−)/TM-*β*-CD, the guest is accommodated 'equatorially' in the host's wide (secondary) rim. TM-*β*-CD macrocycle, far deviating from a regular heptagon, is significantly distorted during the time frame of the simulation. Its primary rim remains 'closed' not allowing to the hydroxyl group of the guest to penetrate the primary methoxy groups 'lid'. Thus, the hydroxyl of the guest is located in the wide rim of the host, hydrogen bonded most of the time with its secondary methoxy groups (Fig. 5c). In the short time intervals where these H-bonds are not observed, the guest adopts an axial orientation opposite to that observed in *cl*/β-CD and *cl*/DM-β-CD inclusion complexes, with its aliphatic chain towards the primary rim of the host and its hydroxyl group fully exposed to the polar solvent. This is not a stable inclusion mode as the hydroxyl of the guest rapidly reforms H-bonds with methoxy groups of the host and the guest turns back to its initial equatorial position.

In order to estimate the binding affinity in the case of the cl/*β*-CD inclusion complex, two separate calculations were made as follows: (i) calculation of the binding energy of guest 1(−) using the system of the two hosts (hostA and hostB) and the 2(+) molecule as receptor and (ii) calculation of the binding energy of 2(+) guest using the two hosts and the 1(−) as receptor. Both calculations resulted in similar values indicating the formation of a stable inclusion complex mainly via van der Waals interactions (Table 2). The binding energy calculated for the 1(−)/DM-*β*-CD inclusion complex (1:1 guest:host stoichiometry) is close to that of cl/*β*-CD, their difference being within the error margins of the method, indicating an also stable inclusion complex. On the other hand, the binding energy calculated for the 1(−)/TM-*β*-CD is significant lower compared to the other two cases confirming the inefficient inclusion of the guest in the hydrophobic cavity of the permethylated *β*-CD.

Table 2
Binding free energies (kcal/mole) resulting from MM/GBSA analysis of the *β*-citronellol inclusion compounds with native and methylated *β*-CDs.

	cl/*β*-CD (i)	cl/*β*-CD (ii)	1(−)/DM-*β*-CD	1(−)/TM-*β*-CD
ΔE_{vdW}	−29.6 ± 2.1	−29.5 ± 2.3	−24.8 ± 2.7	−17.4 ± 4.7
ΔE_{ele}	−1.9 ± 2.0	−2.7 ± 2.8	−2.9 ± 2.7	−3.1 ± 2.9
ΔE_{GB}	13.3 ± 2.4	14.6 ± 2.8	11.0 ± 2.6	10.7 ± 3.2
ΔE_{surf}	−3.8 ± 0.2	−3.8 ± 0.2	−3.4 ± 0.3	−2.7 ± 0.4
ΔG_{gas}	−31.5 ± 2.9	−31.9 ± 3.2	−27.7 ± 3.7	−20.5 ± 5.4
ΔG_{solv}	9.5 ± 2.3	10.7 ± 2.7	7.6 ± 2.6	8.0 ± 3.0
$\Delta G_{(GB)}$[a]	−21.9 ± 2.0	−21.2 ± 1.9	−20.1 ± 2.7	−12.4 ± 4.0
$T\cdot\Delta S$	−17.2 ± 2.3	−17.5 ± 2.2	−16.5 ± 1.7	−16.0 ± 1.7
ΔG_{all}[b]	−4.7 ± 3.0	−3.7 ± 2.9	−3.6 ± 3.2	+3.6 ± 3.3

ΔE_{vdW} = van der Waals contribution from molecular mechanics.
ΔEele = electrostatic energy as calculated by the molecular mechanics force field.
ΔEGB = the electrostatic contribution to the solvation free energy, calculated by GB model.
ΔEsurf = nonpolar contribution to the solvation free energy, calculated by an empirical model.
[a] $\Delta G_{(GB)} = \Delta G_{solv} + \Delta G_{gas}$.
[b] $\Delta G_{(all)} = \Delta G_{(binding)} + (T\cdot\Delta S)$.

4. Conclusions

The X-ray crystal structures of the *cl*/*β*-CD, *cl*/*DM*-*β*-CD and *cl*/*TM*-*β*-CD inclusion complexes confirm the inherent tendency of *β*-citronellol to form inclusion complexes with native and methylated *β*-CDs mainly via the hydrophobic effect and provide accurate molecular parameters of the inclusion geometry.

The crystal structure of *cl*/*β*-CD reveals the encapsulation of a duet of enantiomeric *β*-citronellol molecules in a head-to-head *β*-CD dimer. The inclusion compound crystallizes in the *P*1 space group and the dimers form Intermediate Channels (*IM*) along *c*-axis. The *cl*/DM-*β*-CD and *cl*/TM-*β*-CD inclusion complexes crystallize both in the$P2_12_12_1$space group with 1:1 guest:host stoichiometry. The guest in both complexes is found only with the (−)-*cl* enantiomeric configuration, fully encapsulated axially inside the DM-*β*-CD host cavity with its hydroxyl group protruding from the primary rim of the host and partially encapsulated in the TM-*β*-CD, equatorially accommodated with its alkyl group protruding from the secondary side of the host whose primary side is efficiently blocked by the methoxy groups. The complex units in the case of *cl*/DM-*β*-CD pack along the crystallographic *a*-axis in a head-to-tail manner forming columns of herringbone mode whereas in the case of *cl*/TM-*β*-CD are arranged also in a head-to-tail manner, parallel to the *b*-axis in a screw-channel mode.

MD simulations based on the determined crystal structures of the examined inclusion complexes, showed that in a simulated aqueous environment, although the hydroxyl group of *β*-citronellol switches between different hydrogen bonding partners, the guest maintains the inclusion mode observed crystallographically in every case. Intramolecular (host) and intermolecular (host-guest) hydrogen bonds play significant roles in the relative stabilization of the observed binding modes. Moreover, the lack of mode interconversions may indicate that the binding modes are determined during guest entry in the CD cavity, before incorporation of the complex in the growing crystal. Finally, MM/GBSA-calculations used for comparison of the inclusion complexes binding affinity with each other, indicated that the inclusion of *β*-citronellol in TM-*β*-CD is less favorable than in *β*-CD and DM-*β*-CD.

Appendix A. Supplementary data

Supplementary data related to this article can be found at https://doi.org/10.1016/j.molstruc.2018.02.037.

References

[1] T.M. Katz, J.H. Miller, A.A. Hebert, Insect repellents: historical perspectives and new developments, J. Am. Acad. Dermatol. 58 (2008) 865–871.
[2] M.M.M. Specos, J.J. Garcia, J. Tornesello, P. Marino, M.D. Vecchia, M.V.D. Tesoriero, L.G. Hermida, Microencapsulated citronella oil for mosquito repellent finishing of cotton textiles, Trans. R. Soc. Trop. Med. Hyg. 104 (2010) 653–658.
[3] D. Zamora, S.A. Klotz, E.A. Meister, J.O. Schmidt, Repellency of the components of the essential oil, Citronella, to Triatoma rubida, Triatoma protracta, and Triatoma recurva (Hemiptera: Reduviidae: Triatominae), J. Med. Entomol. 52 (2015) 719–721.
[4] S. Songkro, N. Hayook, J. Jaisawang, D. Maneenuan, T. Chuchome, N. Kaewnopparat, Investigation of inclusion complexes of citronella oil, citronellal and citronellol with β-cyclodextrin for mosquito repellent, J. Inclusion Phenom. Macrocycl. Chem. 72 (2012) 339–355.
[5] A. Huntley, Aromatherapy science: a guide for healthcare professionals, Focus Alternative Compl. Ther. 11 (2006), 260–260.
[6] E.M. Del Valle, Cyclodextrins and their uses: a review, Process Biochem. 39 (2004) 1033–1046.

[7] C. Novák, Z. Éhen, M. Fodor, L. Jicsinszky, J. Orgoványi, Application of combined thermoanalytical techniques in the investigation of cyclodextrin inclusion complexes, J. Therm. Anal. Calorim. 84 (2006) 693–701. J THERM ANAL CALORIM.
[8] APEX 3, SAINT, SADABS Version 2012/1, 1, vol. 2012, Bruker-AXS, Madison, Wisconsin, USA, 2012.
[9] G.M. Sheldrick, SADABS, 2012.
[10] G.M. Sheldrick, A short history of SHELX, Acta Crystallogr. Sect. A. 64 (2008) 112–122.
[11] G.M. Sheldrick, Crystal structure refinement with ıt SHELXL, Acta Crystallogr. Sect. C. 71 (2015) 3–8.
[12] C.B. Hübschle, G.M. Sheldrick, B. Dittrich, ıt ShelXle: a Qt graphical user interface for ıt SHELXL, J. Appl. Crystallogr. 44 (2011) 1281–1284.
[13] A.W. Schuttelkopf, D.M.F. van Aalten, PRODRG: a tool for high-throughput crystallography of protein-ligand complexes, Acta Crystallogr. D Biol. Crystallogr. 60 (2004) 1355–1363.
[14] A. Thorn, B. Dittrich, G.M. Sheldrick, Enhanced rigid-bond restraints, Acta Crystallogr. A. 68 (2012) 448–451.
[15] C.F. Macrae, I.J. Bruno, J.A. Chisholm, P.R. Edgington, P. McCabe, E. Pidcock, L. Rodriguez-Monge, R. Taylor, J. van de Streek, P.A. Wood, *Mercury CSD 2.0 –* new features for the visualization and investigation of crystal structures, J. Appl. Crystallogr. 41 (2008) 466–470.
[16] O.V. Dolomanov, L.J. Bourhis, R.J. Gildea, J.A.K. Howard, H. Puschmann, ıt OLEX2: a complete structure solution, refinement and analysis program, J. Appl. Crystallogr. 42 (2009) 339–341.
[17] D.A. Case, T.E. Cheatham, T. Darden, H. Gohlke, R. Luo, K.M. Merz, A. Onufriev, C. Simmerling, B. Wang, R.J. Woods, The Amber biomolecular simulation programs, J. Comput. Chem. 26 (2005) 1668–1688.
[18] K.N. Kirschner, A.B. Yongye, S.M. Tschampel, J. González-Outeiriño, C.R. Daniels, B.L. Foley, R.J. Woods, GLYCAM06: a generalizable biomolecular force field. Carbohydrates, J. Comput. Chem. 29 (2008) 622–655.
[19] C. Cezard, X. Trivelli, F. Aubry, F. Djedaini-Pilard, F.-Y. Dupradeau, Molecular dynamics studies of native and substituted cyclodextrins in different media: 1. Charge derivation and force field performances, Phys. Chem. Chem. Phys. 13 (2011) 15103–15121.
[20] J. Wang, W. Wang, P.A. Kollman, D.A. Case, Automatic atom type and bond type perception in molecular mechanical calculations, J. Mol. Graph. Model. 25 (2006) 247–260.
[21] D.R. Roe, T.E. Cheatham 3rd, PTRAJ and CPPTRAJ: Software For processing and analysis of molecular dynamics trajectory data, J. Chem. Theor. Comput. 9 (2013) 3084–3095.
[22] W. Humphrey, A. Dalke, K. Schulten, VMD: visual molecular dynamics, J. Mol. Graph. 14 (1996) 33–38.
[23] I. Bill R. Miller, J.T. Dwight McGee, J.M. Swails, N. Homeyer, H. Gohlke, A.E. Roitberg, MMPBSA.py: an efficient program for end-state free energy calculations, J. Chem. Theor. Comput. 8 (2012) 3314–3321.
[24] S. Genheden, U. Ryde, The MM/PBSA and MM/GBSA methods to estimate ligand-binding affinities, Expet Opin. Drug Discov. 10 (2015) 449–461.
[25] D. Mentzafos, I.M. Mavridis, G. Le Bas, G. Tsoucaris, Structure of the 4-ıt tert-butylbenzyl alcohol–β-cyclodextrin complex. Common features in the geometry of β-cyclodextrin dimeric complexes, Acta Crystallogr. Sect. B. 47 (1991) 746–757.
[26] C.R. Groom, I.J. Bruno, M.P. Lightfoot, S.C. Ward, The Cambridge structural Database, Acta Crystallogr. Sect. B. 72 (2016) 171–179.
[27] M. Ceborska, K. Szwed, M. Asztemborska, M. Wszelaka-Rylik, E. Kicińska, K. Suwińska, Study of β-cyclodextrin inclusion complexes with volatile molecules geraniol and α-terpineol enantiomers in solid state and in solution, Chem. Phys. Lett. 641 (2015).
[28] M. Ceborska, Structural investigation of the β-cyclodextrin complexes with linalool and isopinocampheol – influence of monoterpenes cyclicity on the host–guest stoichiometry, Chem. Phys. Lett. 651 (2016).
[29] L. Trollope, D.L. Cruickshank, T. Noonan, S.A. Bourne, M. Sorrenti, L. Catenacci, M.R. Caira, Inclusion of trans-resveratrol in methylated cyclodextrins: synthesis and solid-state structures, Beilstein J. Org. Chem. 10 (2014) 3136–3151.
[30] M.R. Caira, S.A. Bourne, B. Mzondo, Encapsulation of the antioxidant r-(+)-α-lipoic acid in permethylated α- and β-cyclodextrins: thermal and X-ray structural characterization of the 1:1 inclusion complexes, Molecules 22 (2017).